Bioconjugate Chemistry

Article

pubs.acs.org/bc

Site Selective Azo Coupling for Peptide Cyclization and Affinity Labeling of an SH3 Protein

Feng Huang,[†] Yunyu Nie,[†] Fei Ye,*[,‡] Mingjie Zhang,[‡] and Jiang Xia*[,†]

[†]Department of Chemistry, The Chinese University of Hong Kong, Shatin, Hong Kong SAR, China

[‡]Division of Life Science, The Hong Kong University of Science and Technology, Clear Water Bay, Hong Kong SAR, China

Supporting Information

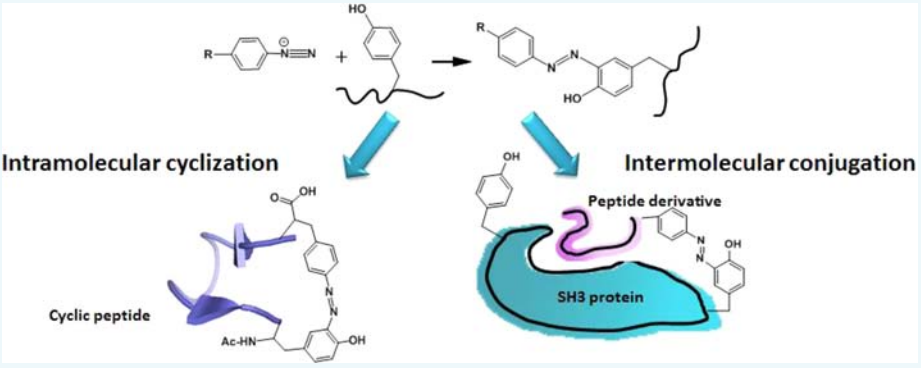

ABSTRACT: A key challenge in bioconjugation is to control the site selectivity of the reaction. Chemical reagents often react with proteineous chemical groups without showing preference to their location or microenvironment in the protein; to confine the reaction to an amino acid at a specific site, one needs to distinguish this residue from others despite their identical chemical properties. Here, we report a strategy that utilizes proximity-driven reactivity to achieve site selective azo coupling between tyrosine and aryldiazonium. A phenylalanine analogue with an aryldiazonium moiety at its side chain was incorporated into a synthetic peptide and was found to react only with tyrosine in its vicinity but also to remain inert to others that are not immediately adjacent, a property attained by fine regulation of the electronic effect of the substituent on the aryl ring. Proximity-driven intramolecular azo coupling was showcased in cyclization of a β-hairpin peptide, structural features of the azo linked cyclic peptide was elucidated by NMR, and intermolecular azo coupling was achieved between an SH3 protein Abl-SH3 and its polyproline peptide ligands at specific tyrosine residues. This approach is generally applicable to develop covalent affinity labels for SH3 proteins because of the high occurrence rate of tyrosine at the peptide-binding site of SH3 proteins.

INTRODUCTION

To effectively build covalent bonds with proteins, bioconjugation reagents having optimal chemical reactivity for proteineous chemical groups have been developed.[1] Controlling the regioselectivity (or site selectivity) of the reaction on proteins is more challenging. In other words, it is difficult to devise a bioconjugation reagent that only engages one particular residue in reaction leaving others of the same kind unreacted. Nature, however, does not solely depend on chemical reactivity to differentiate one residue from another; the flanking amino acids often dictate the reaction site. For instance, some enzymes endow one residue (active site residue) with outstanding chemical reactivity by creating a unique microenvironment around it; substrate binding then juxtaposes the active site residue in the vicinity of the substrate to induce a chemical reaction at the precisely controlled position of the substrate.[2] Inspired by this "bind-then-react" mode of action, we and others have exploited the strategy called "affinity-guided covalent conjugation," "proximity-induced reactivity," or "ligand-directed affinity labeling" and successfully implemented it in cysteine-specific conjugation to covalently and site-specifically cross-link nonenzyme proteins and their ligand derivatives.[3−8]

One limitation of cysteine-specific chemistry, however, is the low occurrence of cysteine residues in proteins, ∼1.9%, inclusive of those that have formed disulfide bonds.[9] Cysteine residues that are exposed on the surface of natural proteins, not forming disulfide bonds, adjacent to the ligand binding site, and amenable for covalent conjugation are uncommon. Take the SRC Homology 3 domain (SH3) proteins as an example: only one out of over 300 SH3 structures from the Protein Data Bank contains cysteine close to the peptide-binding pocket that one can build a covalent bond with. Moreover, out of 10,665 SH3 domains from the Pfam database,[10] only 86 (0.8%) potentially contain a cysteine at the peptide-binding site. Tyrosine has a much higher occurrence rate, 3.2%, and is often found at the

Received: April 28, 2015
Revised: June 26, 2015
Published: July 2, 2015

DOI: 10.1021/acs.bioconjchem.5b00238
Bioconjugate Chem. 2015, 26, 1613−1622

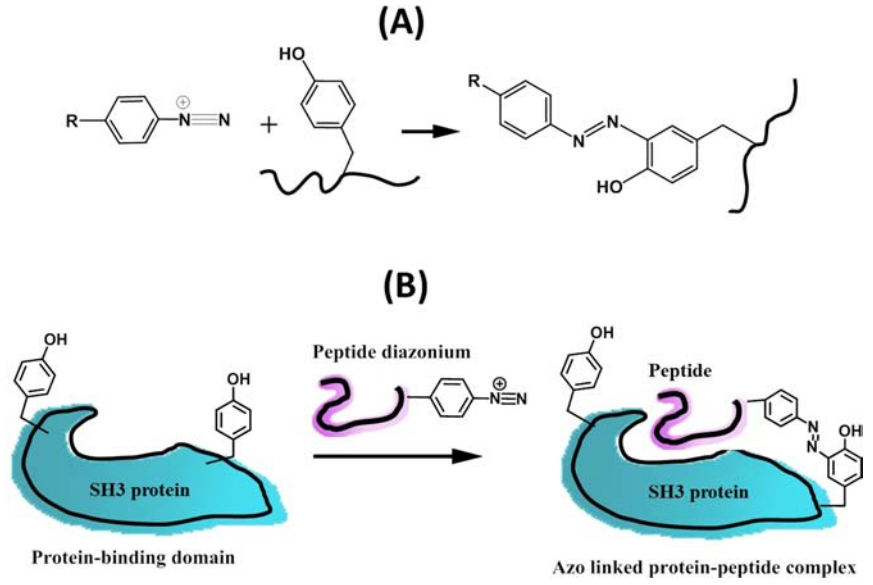

Figure 1. Proximity-induced azo coupling reaction for site selective tyrosine conjugation. (A) Diazonium salt reacts with tyrosine through an electrophilic aromatic substitution reaction to establish an azo linkage, which shows characteristic UV absorption at 350 nm. (B) Protein-peptide binding interaction brings a weakly reactive diazonium moiety to the vicinity of a tyrosine residue to result in an azo coupling reaction. Tyrosine at a different position of the protein will not react.

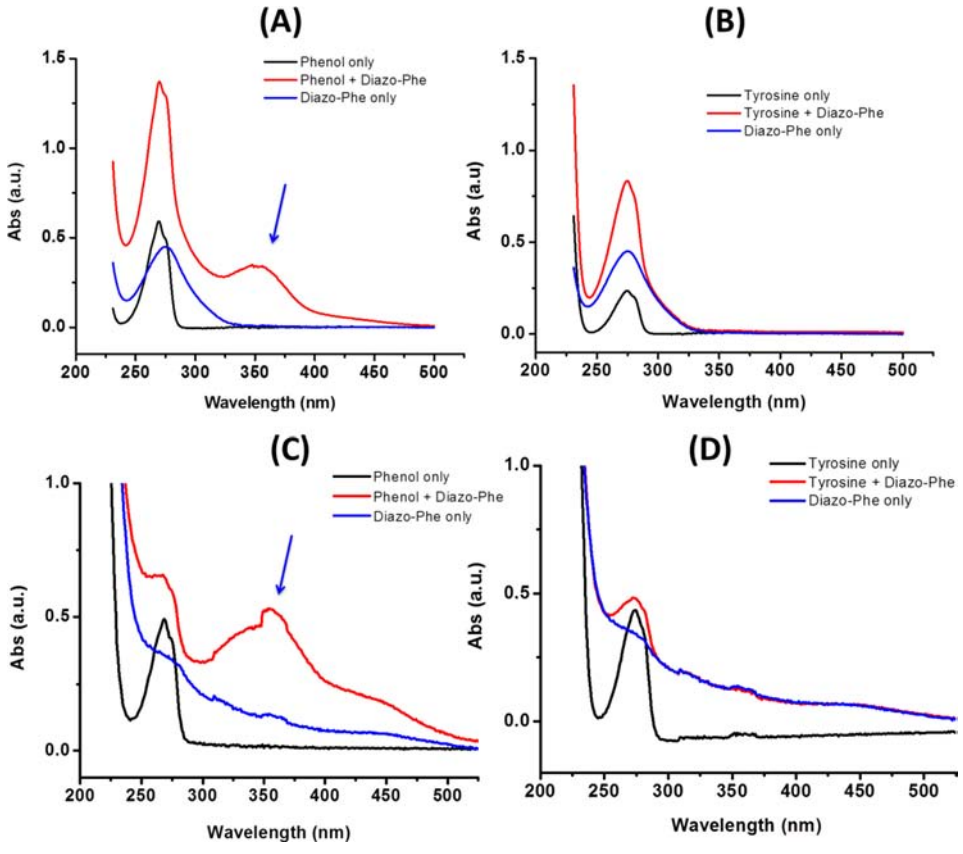

Figure 2. Diazo-Phe reacts with phenol at pH 4.5 (A) and at pH 7.4 (C) but not with tyrosine at pH 4.5 (B) or at pH 7.4 (D) monitored by UV–vis absorption spectroscopy. The arrow indicates the **diazo-Phe**/Phenol azo coupling product showing a characteristic absorption peak at 350 nm. Reactants of 1 mM each were mixed in citrate-PBS buffer (pH 4.5 or pH 7.4) and incubated at room temperature for 3 h.

interface of protein–protein complexes. Overall, 8,599 out of a total of 10,749 SH3 domains (80%) contain at least one Tyr residue at residues #7 and #52, both adjacent to and pointing toward the bound peptide (the residue numbering follows the sequence of human Abl-SH3 domain, PDB ID 1BBZ[11]). Tyrosine-specific site selective conjugation can therefore be applied to more proteins than the cysteine-specific reaction.

Aryldiazonium compounds are known to undergo an electrophilic aromatic substitution reaction with the side chain phenol of tyrosine to give an azo compound (hence its

DOI: 10.1021/acs.bioconjchem.5b00238
Bioconjugate Chem. 2015, 26, 1613–1622

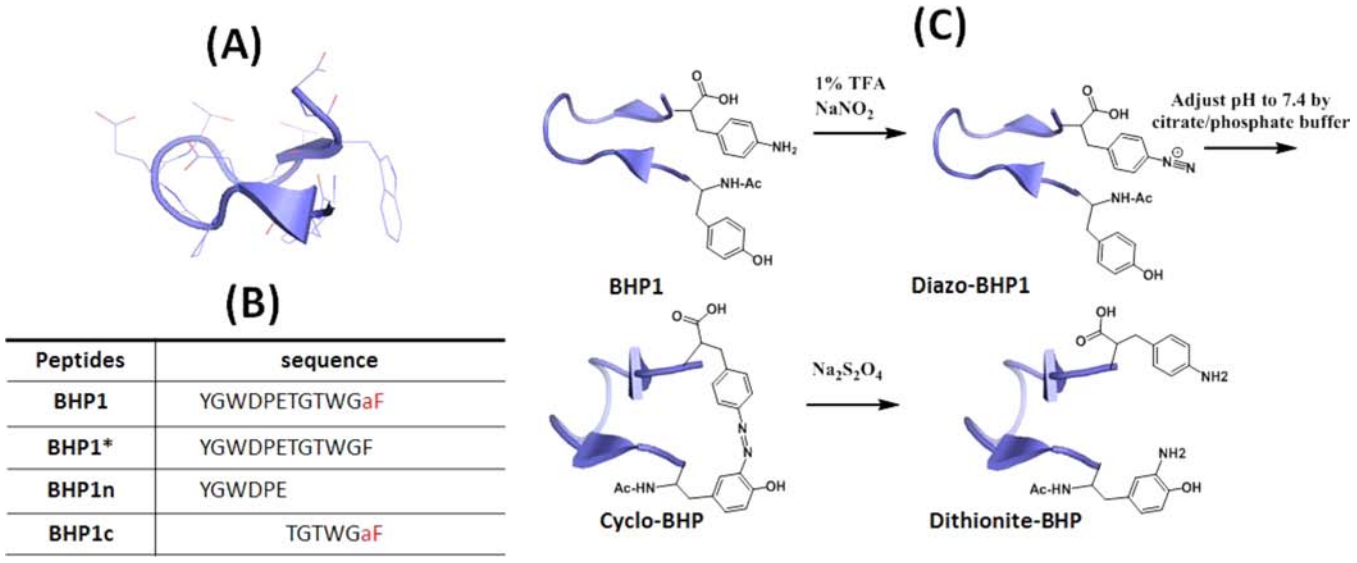

Peptides	sequence
BHP1	YGWDPETGTWGaF
BHP1*	YGWDPETGTWGF
BHP1n	YGWDPE
BHP1c	TGTWGaF

Figure 3. Intracellular cyclization of a β-hairpin peptide through proximity-induced reactivity. (A) The structure of chignolin shows a stable β-hairpin structure in solution (PDB ID 1UAO). (B) The sequences of **BHP1**, **BHP1***, **BHP1n**, and **BHP1c**. The residue **aF** denotes *p*-amino phenylalanine. (C) The reaction scheme of diazotization, azo coupling, and cleavage of the azo bond.

name azo coupling) (Figure 1A).[12−15] Electron-withdrawing substituents in para position regarding the azo group increase the aryldiazonium ions' electrophilicity so that diazonium coupling occurs with phenols and phenolic ethers, such as anisole, which have relatively low reactivity.[14,16] Otherwise, the unsubstituted benzenediazonium cation only reacts with strongly activated aromatic compounds, such as phenolates, requiring higher pH to deprotonate tyrosine to allow for the reaction. However, Tsao and co-workers showed that deactivated aryldiazoniums (with electron donating groups such as -NHCOCH$_3$, -CH$_3$, and -H at the para position of the diazo group) react with the 2-naphthol analogue of the tyrosine but not with the phenol group on tyrosine at neutral pH.[16] Taken together, we envision that there should exist a narrow reactivity window for the substituent effect of aryldiazonium. We therefore seek to develop modestly active aryldiazonium compounds that do not react with tyrosine when simply mixed but react when aryldiazonium and tyrosine are brought into close vicinity by biological interaction, a *sine qua non* of site selective azo coupling (Figure 1B).

RESULTS AND DISCUSSION

Synthesis of Diazonium Compounds with Moderate Reactivity. Electron withdrawing groups at the aryldiazonium ring are known to activate the diazonium for electrophilic aromatic substitution,[17] and activated diazonium compounds spontaneously couple with tyrosine at its phenolic ring. Changing the electronic property of the substituent will fine-tune the reactivity of aryldiazonium.[14,16] We therefore proposed that diazophenylalanine (**diazo-Phe**, which is a diazonium derivative of phenylalanine attained from the reaction of aminophenylalanine, **amino-Phe**, with sodium nitrite under acidic conditions) should have moderate reactivity due to the weak electron donating effect of the -CH$_2$R group at the para position of the diazo group. In a pilot experiment, we found that **diazo-Phe** can react with phenol at both pH 4.5 and pH 7.4, supported by the appearance of a new peak at around 350 nm in UV−vis spectroscopy, characteristic of an azo linked product (Figure 2). However, **diazo-Phe** did not react with tyrosine (Figure 2), indicating that the reactivity of the phenolic side chain of tyrosine drops below the threshold of the azo coupling reaction with **diazo-Phe** in solution. In other words, there does exist a narrow reactivity window where the coupling between **diazo-Phe** and tyrosine can take place if the condition is slightly favored for activation. We envision that the proximity effect may play a role of "the slight activation": when positioned in close vicinity, **diazo-Phe** is expected to react with tyrosine to give the azo coupling product at pH 7.4 and room temperature.

Intramolecular Cyclization of a β-Hairpin Peptide. To prove this hypothesis, we first sought to cyclize the N and C termini of a β-hairpin peptide (BHP) through an azo coupling reaction, taking advantage of the preformed secondary structure, which positions the two ends in close distance. Chignolin (with a sequence of ac-GYDPETGTWG; ac- denotes acetyl group) is a designed peptide that adopts a β-hairpin structure in solution.[18−21] Hairpin structure confines the N terminal tyrosine and C terminal tryptophan into close proximity, with the distance between the two β carbons measuring 5.4 Å (PDB ID 1UAO) (Figure 3A).[18] It then can serve as a template for the proximity-driven reaction. **BHP1** peptide ac-YGWDPETGTWG(aF) with Tyr at the N terminus and **amino-Phe** at the C terminus was then synthesized (the Y → W mutation is underlined; **aF** denotes aminophenylalanine **amino-Phe**). The $\pi-\pi$ stacking interaction between the N terminal Trp and C terminal Trp stabilizes the β-hairpin structure.[22] After converting **amino-Phe** to **diazo-Phe** by sodium nitrite in acid through diazotization, the solution was quickly buffered to pH 4.5 or pH 7.5 by citrate buffers of different compositions to initiate the azo coupling reaction. Peptide **BHP1***, ac-YGWDPETGTWGF, with a Phe instead of **amino-Phe** at the C terminus was also synthesized as a negative control. As a control of reactivity-driven reaction, the sequence was also split into two separate peptides, **BHP1n** (with a sequence of ac-YGWDPE) and **BHP1c** (with a sequence of ac-TGTWG(aF)) having the two reactive moieties **diazo-Phe** and Tyr located on each of the two peptides (Figure 3B). We expect that diazotization will convert **amino-Phe** to **diazo-Phe** in the peptide and that proximity will drive the cyclization of

DOI: 10.1021/acs.bioconjchem.5b00238
Bioconjugate Chem. 2015, 26, 1613−1622

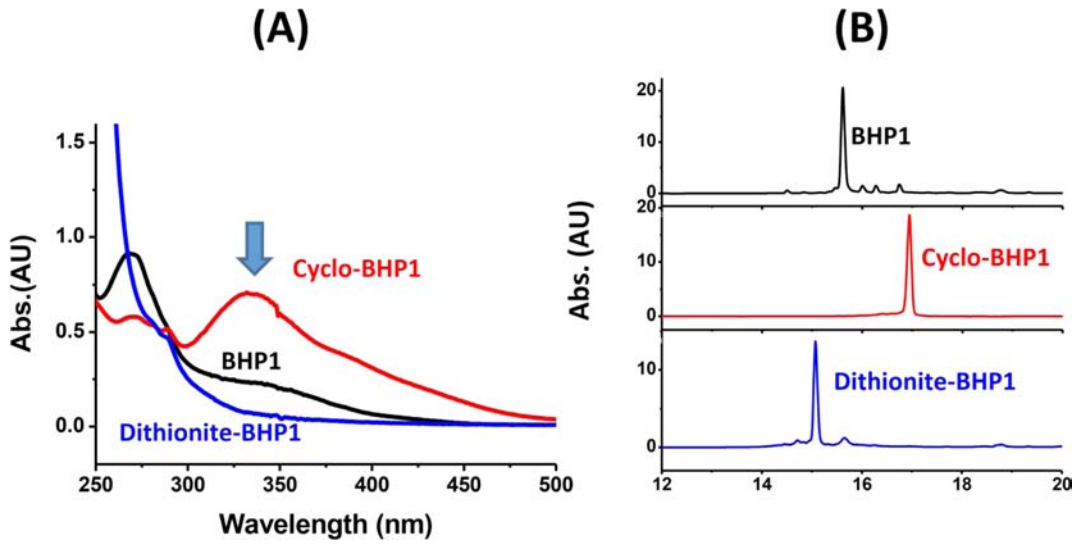

Figure 4. Products of **BHP1** cyclization. (A) Azo coupling product **cyclo-BHP1** showed a characteristic absorption peak at 350 nm in UV−vis spectroscopy, but **BHP1** and **dithionite-BHP1** did not show this absorption peak. (B) **BHP1**, **cyclo-BHP1**, and **dithionite-BHP1** showed different retention times on reverse HPLC. Quantitative conversion in each step could be clearly seen from HPLC traces.

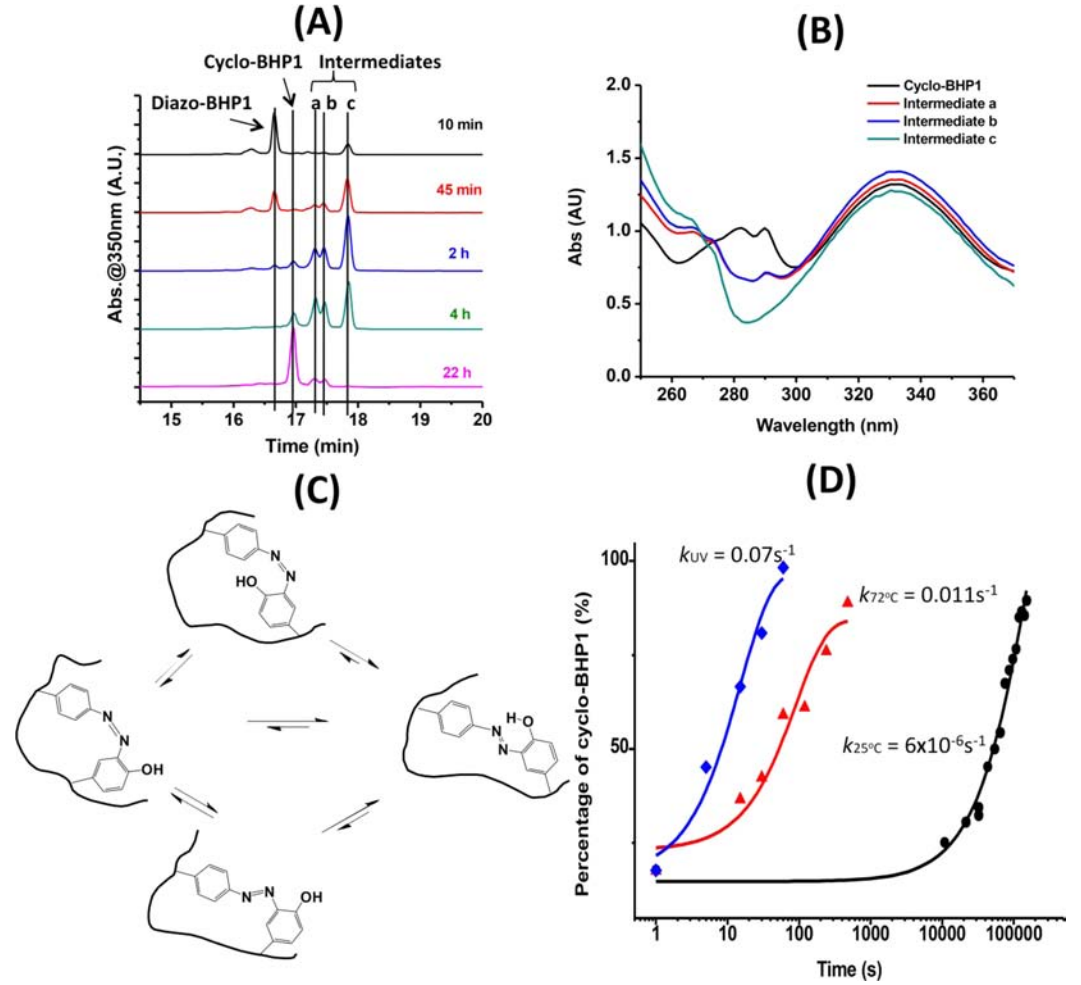

Figure 5. Intermediates of **BHP1** cyclization at room temperature. (A) Peptide peaks a, b, and c at retention times 17.3, 17.4, and 17.8 min emerged and then disappeared during the course of the reaction concomitant with the growing product peak. (B) UV−vis spectra of all four peaks showed characteristic absorption maximum at 350 nm. The spectra were recorded directly from the diode-array detector during HPLC runs. (C) A plausible mechanism to explain the conformational rearrangement during the course of the reaction (the exact structures of the intermediates are not known; the structures drawn here are for reference only). (D) Higher temperature and UV irradiation markedly speeded up the conformal rearrangement. The *Y*-axis shows the percentage of **cyclo-BHP1** in the total amount of cyclic peptides (a + b + c + **cyclo-BHP1**).

DOI: 10.1021/acs.bioconjchem.5b00238
Bioconjugate Chem. 2015, 26, 1613−1622

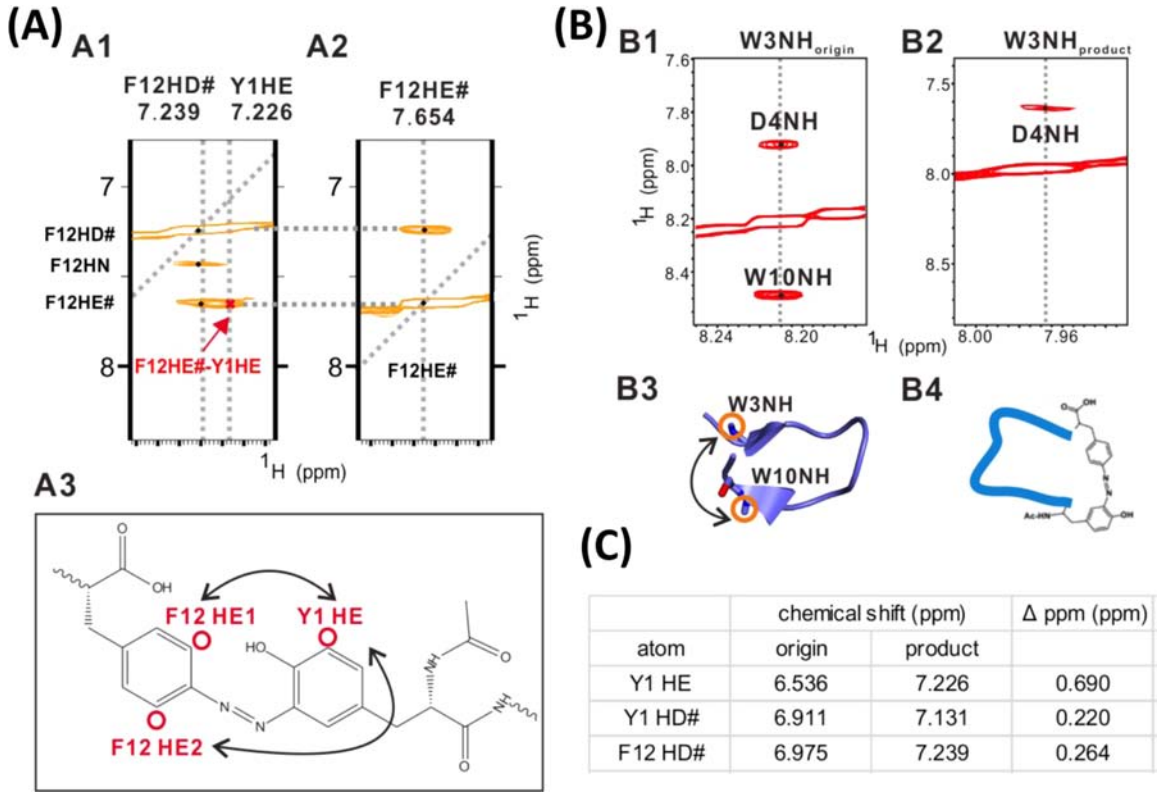

	chemical shift (ppm)		Δ ppm (ppm)
atom	origin	product	
Y1 HE	6.536	7.226	0.690
Y1 HD#	6.911	7.131	0.220
F12 HD#	6.975	7.239	0.264

Figure 6. NMR based structural analysis of **BHP1** cyclization peptide. (A) Selected strips from the 2D ^{1}H−^{1}H NOESY spectrum of **cyclo-BHP1**, showing NOE between the side chain of Y1 and F12 aromatic rings (A1 and A2). The detailed atom information is shown (A3). (B) Selected strips from the 2D ^{1}H−^{1}H NOESY spectrum of **BHP1** peptide and **cyclo-BHP1**, showing that the beta-hairpin conformation is disrupted in the **cyclo-BHP1**. Both the sequential (the NOE between backbone amides of W3 and D4) and beta-hairpin NOE between the backbone amides of W3 and W10 can be found in the **BHP1** control peptide (B1). The amides of W3 and W10 are shown in B3 to be consistent with the beta-strand conformation. The beta-hairpin NOE between W3 and W10 disappears in the **cyclo-BHP1**, indicating that the beta-hairpin is disrupted in the sequential and beta-sheet NOEs in the original peptide (B2). Only sequential NOE can be found in the **BHP1** cyclized peptide indicating that the product is still sequentially linked and that the beta-hairpin structure is disrupted (B2). The residues form much flexible conformations without any secondary structure (B4). (C) Chemical shifts showing the conformational changes of **BHP1** upon cyclization.

the **BHP1** peptide through azo coupling to yield **cyclo-BHP1**. The presence of an azo linkage in **cyclo-BHP1** could also be verified by reaction with sodium dithionite to cleave this bond (Figure 3C).[1,23,24] In the mixture of **BHP1n** and **BPH1c**, Tyr and **diazo-Phe** encounter each other through random diffusion without any structural confinement, which also means the disappearance of the proximity effect.

The reaction systems were first examined by UV−vis spectroscopy to monitor the progress of the reaction. We found that only the **BHP1** reaction system gave a new peak at 350 nm, suggesting the formation of the azo product **cyclo-BHP1** (Figure 4A). The two control systems, **BHP1*** or a **BHP1n** + **BHP1c** mixture, did not give rise to a new peak at 350 nm. The product **cyclo-BHP1** was also confirmed by mass spectroscopic analysis ($[M + H]^+$ calcd 1483.6, obsd 1483.4; $[M + 2H]^{2+}$ calcd 742.3, obsd 742.3; 1 Da lower than the **diazo-BHP1**) (Figure S1, Supporting Information). Sodium dithionite ($Na_2S_2O_4$) cleaved the azo coupling bond and resulted in decyclization of the **cyclo-BHP1** to give **dithionite-BHP1**. All three compounds, **BHP1**, **cyclo-BHP1**, and **dithionite-BHP1** can be well separated on reverse phase HPLC (Figure 4B). Two conclusions can be drawn from this experiment. (1) **Amino-Phe** in the sequence of the peptide can be converted to **diazo-Phe** by $NaNO_2$ treatment in acid. This reaction does not modify other residues in the peptide including Tyr, Gly, Trp, Asp, Phe, Glu, and Thr. (2) Proximity of **amino-Phe** and Tyr, imposed by the turn structure, induced the azo coupling reaction. When the two reactive groups were simply mixed in solution (at μM concentration), the azo coupling reaction did not occur. This conjugation reaction therefore is in accord with the principle of proximity-driven reactions. Besides tyrosine, we also examined the reaction between benzenediazonium and a few other amino acids, and discovered that diazonium reacted with histidine, giving two peaks which might correspond to azo coupling at different positions of imidazole (Figure S2D, Supporting Information). We also screened the stability and reactivity of a set of 8 BHP peptides by replacing the reacting Tyr with His, Lys, Arg, Ser, Cys, Phe, and Trp (Figure S2, Supporting Information). We observed that **diazo-Phe** containing BHP peptides showed higher stability in aqueous solution at pH 4.5. In contrast, at neutral pH in aqueous solution, the azo coupling reaction could readily happen in a tyrosine or histidine specific fashion, but those without a tyrosine/histidine residue at the specific position rapidly degraded (Figure S2K, Supporting Information).

Besides the reactant **diazo-BHP1** and the products **cyclo-BHP1** and **dithionite-BHP1**, we also surprisingly found three peaks on HPLC during the course of the reaction (peaks a, b, and c, in Figure 5A). With retention times different from those of either the reactant or the product, the peaks emerged, increased to their maximal heights, and finally diminished with

DOI: 10.1021/acs.bioconjchem.5b00238
Bioconjugate Chem. 2015, 26, 1613−1622

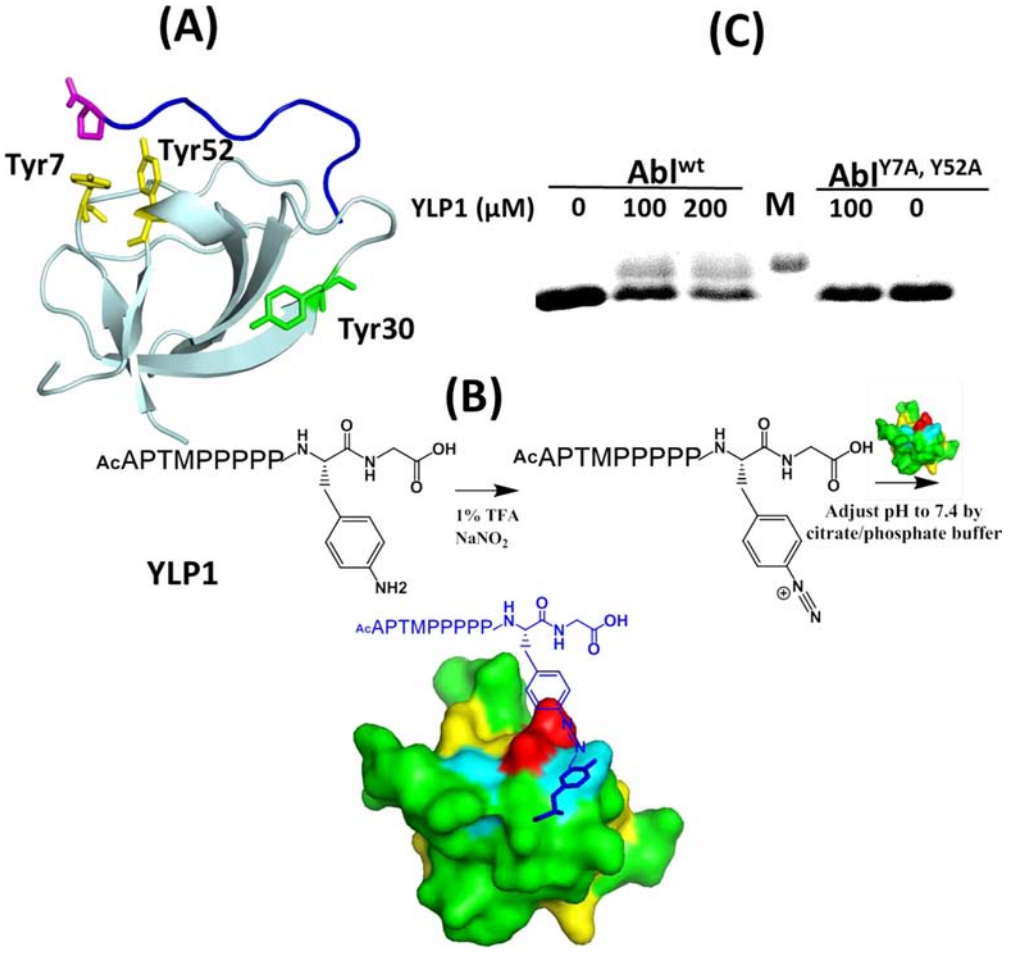

Figure 7. Intermolecular protein−peptide conjugation. (A) Crystal structure of Abl-SH3 in complex with its peptide ligand (PDB ID 1BBZ). The tyrosine residues Tyr7 and Tyr52 that are adjacent to the peptide binding sites are highlighted in yellow, and Tyr30, far away from the peptide binding site, is highlighted in green. (B) Schematic illustration of the intermolecular conjugation reaction. (C) **Diazo-YLP1** peptide covalently conjugated with wild type Abl-SH3, but not the mutant. M, molecular weight markers.

the concomitant increase of the product peak. So they are intermediates of the reaction. Interestingly, all these species showed molar mass identical to that of **cyclo-BHP1** on mass spectra and absorption maxima at 350 nm in UV−vis spectra, suggesting that they all contain the azo linkage (Figures 5B and S1, Supporting Information). We therefore hypothesized that these peaks correspond to different conformers of **cyclo-BHP1** and that the final product **cyclo-BHP1** likely adopts the most stable conformation (Figure 5C). We observed that it took 3 h for the original **BHP1** to be fully converted to azo products, though being a mixture of peaks a, b, c and **cyclo-BHP1**, at room temperature, was indicated by the disappearance of the **BHP1** peak on HPLC. Taking advantage of this characteristic, we first converted **BHP1** to an azo-linked cyclic mixture by continuing the azo coupling reaction for 3 h at room temperature (HPLC analysis confirmed the disappearance of the reactant peak) and then set out to explore the isomerization of the mixture of azo-linked cyclic forms by varying the physical conditions of the reaction solution and simultaneously observing the conversion of the peaks. Although direct evidence for the structure of other conformers was not obtained, we observed that temperature increase and UV irradiation could markedly expedite the conversion of the intermediates to the final product. The conversion of the intermediates to the final conformer took tens of hours to achieve full completion at 25 °C, whereas at higher temperature (72 °C), it finished within 10 min. UV irradiation of 302 nm was even more effective, driving the full conversion of the intermediate peaks to the final peak within 1 min of treatment (Figure 5D and Figure S3, Supporting Information). This evidence aligns with our hypothesis. Although normally very rapid, isomerization of the azo linkage was markedly slower in the **cyclo-BHP1** system at room temperature and in the absence of UV irradiation, as the rigid peptide backbone retarded the otherwise rapid isomerization of the azo linkage. The intermediates we observed could also be attributed to the local minima of various conformational isomers of the peptide because the peptide likely underwent a large conformational alteration after cyclization (evidence shown below). We also observed that the conversion of **diazo-BHP1** to **cyclo-BHP1** at 4 °C followed a different mechanism likely due to the different folding of the **BHP1** peptide at 4 °C as compared to that at room temperature (Figure S4, Supporting Information). The reaction routes are therefore a joint effect of both peptide folding and isomerization of the azo linkage.

Structural Alteration Imposed by Cyclization. To provide further support on azo linkage mediated cyclization of **BHP1** and as to whether azo coupling affects the secondary structure of the peptide, we next sought structural evidence by solution NMR spectroscopy. We first looked for the evidence

DOI: 10.1021/acs.bioconjchem.5b00238
Bioconjugate Chem. 2015, 26, 1613−1622

of azo linkage in **cyclo-BHP1**. A NOE (Nuclear Overhauser Effect) between the Y1 HE and F12 HE# (Figure 6A1, A2, and A3) was found from the 2D $^{1}H-^{1}H$ NOESY spectrum of **cyclo-BHP1**, which clearly indicated a close distance between these two hydrogen atoms in **cyclo-BHP1**, around 5 to 8 Å. (HE# refers to either HE1 or HE2 collectively in Figure 6A3, because these two hydrogen atoms cannot be differentiated from NMR data. Y1 denotes the first tyrosine residue, whereas F12 represents the **diazo-Phe** residue.) In contrast, this NOE cannot be found in the **BHP1** control peptide (uncyclized form), indicating the formation of azo linkage in **cyclo-BHP1**, which links the two side chains of Y1 and F12 in close proximity. However, despite the clear assignment of this NOE, we cannot tell exactly which conformation of the final stable **cyclo-BHP1** is adopted (Figure 5C) because of the lack of sufficient information to differentiate the F12 HE1 from HE2. This result is consistent with the previous MS, UV−vis, and HPLC results indicating that the azo linkage has successfully formed between tyrosine and **diazo-Phe**.

We then looked for whether the overall structure of the β hairpin peptide was affected by azo linkage of the N and C termini. Along this line, clear sequential NOE was first found in the **cyclo-BHP1** (Figure 6B2 and Figure S5, Supporting Information), supporting the notion that the peptide was not broken upon the cyclization. (Sequential NOE means the residue on the n + 1 site always can have sequential NOE with the residue on the n site, which is only determined by sequence. However, when the sequence is broken, the NOE on the broken site will disappear.) Furthermore, we found the NOE between the backbone amides of W3 and W10 (Figure 6B1), proving that the uncyclized **BHP1** peptide adopts a characteristic β hairpin structure (Figure 6B3), consistent with the previous report.[18] (Other NOEs that support the β hairpin conformations can also be found but are not shown in Figure 6.) However, these NOEs in uncyclized **BHP1** peptide characteristic of β hairpin structure were missing in **cyclo-BHP1**, indicating that the β hairpin structure is lost after azo coupling cyclization (Figure 6B2). In fact, all of the NOEs characteristics of the secondary structure in **BHP1** are lost in **cyclo-BHP1**, suggesting that apart from the residues involved in azo coupling (Y1 and F12), the other residues adopt a flexible conformation (Figure 6B4). Moreover, we observed marked differences of chemical shifts of several hydrogen atoms as we compared the peptide structure before and after azo cyclization (Figure 6C). As larger chemical shift differences indicate larger structural change, this observation further supports the drastic conformational change of **BHP1** after cyclization. Taken together, our NMR analysis clearly indicated that (1) azo linkage was formed between tyrosine and **diazo-Phe** and that (2) azo coupling-based cyclization imposed a drastic structural change to the peptide, forcing the distortion of β hairpin structure to a disordered structure, which might also be the cause of the intermediates.

Intermolecular Protein−Peptide Conjugation: Covalent Labeling of an SH3 Protein. We finally performed an intermolecular bioconjugation reaction by covalently linking a tyrosine-containing protein with the diazonium derivative of its ligand peptide through azo coupling. An SH3 protein Abl-SH3 was chosen as our example.[11,25,26] The Abl-SH3 domain in its natural form contains tyrosine at position 7, which directly points toward the C terminal proline of the polyproline peptide APSYSPPPPP.[11,27−31] The distance between the β carbon of Tyr7 of Abl-SH3 and the Pro of the peptide is measured to be 3.8 Å (Figure 7A).[11] Notably, there is another tyrosine residue, Tyr52 that is nearby, with the distance between its β carbon and that of Pro being 6.8 Å. We then synthesized a reactive peptide **YLP1**, with a sequence of ac-APTMPPPPPP(aF)G based on ligand p50; APTMPPPPPP is a micromolar affinity ligand of Abl-SH3.[31] After diazotization of **amino-Phe** to **diazo-Phe**, the peptide was neutralized to pH 7.4 and mixed with wild type Abl-SH3 protein to allow for the reaction to take place (Figure 7B). A protein band with slightly higher molecular weight can be seen on denaturing SDS−PAGE, indicating the formation of a covalently linked complex (Figure 7C). **YLP1** did not react with a Y-to-A double mutant of Abl-SH3, despite the presence of another tyrosine residue at position 30 in the protein. The intermolecular reaction therefore abided by the principle of affinity-guided conjugation. Both single mutants Abl-SH3^{Y7A} and Abl-SH3^{Y52A} showed much weaker reaction with **YLP1** than the wild type Abl-SH3, concluding that Tyr7 and Tyr52 both are the reactive sites for diazonium (Figure S6C, Supporting Information). In view of the relatively low reaction efficiency, we also examined the conjugation reactions by varying the pH of the solution and the temperature at which the reaction was performed. We observed that peptide diazonium tends to destabilize the protein and cause precipitation. Although higher pH and higher temperature promoted the conjugation reaction, these conditions also destabilized the protein and caused protein precipitation from the solution. These two counteracting factors restrict the overall maximal efficacy of the conjugation to be at around 30% (Figure S6, Supporting Information).

■ CONCLUSIONS

We tuned the long-known azo coupling reaction for proximity-induced reaction with tyrosine, providing a new solution instead of a new reaction for site selective conjugation. Although histidine is also a reactant for diazonium under reactivity-driven conditions, structure-based ligand design can facilitate precise targeting of a given tyrosine in a peptide or protein. Therefore, the combination of chemical reactivity and spatial confinement dictates the accuracy of site selectivity during the bioconjugation reaction. We showcased that a diazonium-containing peptide can covalently label an SH3 protein, Abl-SH3, by an azo coupling reaction with the highly conserved tyrosine residues located at the peptide-binding site of the SH3 protein. This approach can be extended to develop covalent affinity labels for peptide-binding proteins, such as SH3 domains, under the condition that one can find tyrosine residues at their peptide-binding sites.

This approach, however, has intrinsic limitations for intracellular applications. One restriction is the need of an unnatural group, which requires either a presynthesized chemical entity to be delivered into the cell[32,33] or the genetic incorporation of an unnatural amino acid in the protein. As both efforts are nontrivial, admittedly for some applications the azo coupling reaction is inferior to the ones that only use natural amino acids for covalent linkages, for example, the SpyTag-spyCatcher method.[34−36] The stability of the diazonium moiety poses another limitation. While intracellular peptide cyclization proceeded to full completion, intermolecular conjugation suffered from a moderate yield. In the former system, once the diazonium moiety was generated, it immediately reacted with the nearby tyrosine, but in protein−peptide conjugation, after the peptide diazonium salt was generated, it needed to be mixed with the protein solution

DOI: 10.1021/acs.bioconjchem.5b00238
Bioconjugate Chem. 2015, 26, 1613−1622

to allow for an azo coupling reaction to take place. The delay in the subsequent reaction and the change of physical environment resulted in rapid deterioration of the peptide diazonium salt, likely in the form of precipitates as shown in HPLC and SDS−PAGE, and rendered the reaction uncontrolled. Notwithstanding that the low stability of diazonium salts leads to low yield in intermolecular conjugation and the intracellular applications, proximity-induced azo coupling still represents a useful new member in the toolbox of bioconjugation reactions.

Our work presents another example that proximity-induced reaction leads to sequence- and site-selectivity in protein modification. Many solution reactions have been tailored to occur only in a proximity-induced fashion. For example, Ball and co-workers reported the activation of a specific aromatic side chain with a dirhodium metallopeptide catalyst that is positioned in the vicinity of the reactive site[37,38] (also extensively reviewed in ref 39). Hamachi and co-workers pioneered ligand-guided tosyl chemistry[40,41] and catalytic target-selective modification using ligand-tethered *N*,*N*-dimethylaminopyrine (DMAP) catalysts.[42,43] Sato and Nakamura developed a ligand-directed catalytic oxidative radical addition reaction based on single-electron transfer with a ruthenium photocatalyst.[44] Howarth and co-workers engineered electrophilic affibodies by appending an acrylamide moiety at selected positions of affibodies to react with cysteine, lysine, or histidine in proximity.[45] Taunton and co-workers also reported irreversible kinase inhibitors which form a covalent bond with a proximal cysteine that is poorly conserved.[46] These examples as well as many others demonstrated that locally positioned reactive groups or catalysts of various chemical properties can activate nonreactive natural side chains to result in sequence- and site-selective covalent conjugations on proteins. The majority of these reactions were tested on purified proteins in test tubes or on the surface of mammalian cells, where the reaction conditions are relatively simple. We envision that many of these proximity-driven reactions can take place inside living cells or even in tissues to redirect cell signals or reconstruct protein assemblies. These explorations toward these applications are underway in our laboratory and will be reported in due course.

MATERIALS AND METHODS

Synthesis of Diazo-phenylalanine (Diazo-Phe) Containing Peptides. The unnatural amino acid **amino-Phe** was incorporated into the peptide sequence during solid phase peptide synthesis using Fmoc-4-(Boc-amino)-L-phenylanine-OH (Chem-Impex International, Inc. USA). **Amino-Phe** containing peptides (2 mM) were converted to **diazo-Phe** containing peptides by treating with sodium nitrite (0.1 M) in 1% TFA in water for 30 min on ice. Lysine, arginine, asparagine, and glutamine were omitted from the peptide sequence, and the N terminal amino group was protected to avoid side reactions during diazotization.

Beta-Hairpin Peptide Cyclization. The peptide **BHP1** ac-YGWDPETGTWG(aF) was synthesized, purified and then diazotized by $NaNO_2$ in acidic solution. The diazo containing peptide was then diluted into pH 7.4 (182 mM Na_2HPO_4, 9 mM citrate), and the final concentration of the reactant was 20 μM. The reaction was set at room temperature (25 °C), and the conversion ratio was monitored at different time points by reverse phase HPLC and UV−vis spectroscopy. After completion of the cyclization, $Na_2S_2O_4$ (final concentration 0.1 M) was added as reducing reagent to cleave the azo linkage and decyclize **cyclo-BHP1** for 1 h at room temperature.

NMR Analysis of Cyclo-BHP1. Peptides **BHP1** and **cyclo-BHP1** were prepared for structural analysis in aqueous solution by NMR spectroscopy (unlabeled peptides in 90% H_2O/10% D_2O). The concentrations of the NMR samples were around 1.0 mM, and pH values of the samples were adjusted to 7.0. All NMR spectra were recorded on a Varian Inova 750-MHz spectrometer equipped with an actively z-gradient shielded triple-resonance probe at 273 K. 2D 1H−1H TOCS, and NOESY were obtained. Mixing times of 300 ms were used in the NOESY experiments. NMR data were processed using the nmrpipe software package[47] and analyzed using SPARKY3.[48]

Protein Expression, Purification, and Characterization. Human wild type Abl-SH3 domain and its mutants Abl-$SH3^{Y7A}$, Abl-$SH3^{Y52A}$, and Abl-$SH3^{Y7A/Y52A}$ were constructed into pGEX6p1 plasmids with the restriction site NdeI and XhoI. The plasmids were transformed into *E. coli* BL21. Protein expression was induced by IPTG (final concentration was 0.1 mM) when OD_{600} of the culture reached 0.6. The expressed proteins were purified using GST-tag binding beads, column bound GST-fusion protein was removed from the resins by PreScission Protease (GE, USA), and the purity of the protein was confirmed by SDS−PAGE.

Azo Coupling between the SH3 Protein and Peptide. The peptide **YLP1** ac-APTMPPPPP(aF)G was synthesized and purified. After 30 min of diazotization on ice, the peptide was mixed with SH3 protein solutions and phosphate buffer (pH 7.4, 182 mM Na_2HPO_4, 9 mM citrate), and allowed to react at room temperature for 2.5 h. The final concentrations of the proteins and the peptide were 20 μM and 100 μM, respectively. Tricine SDS−PAGE (described in the literatue[49]) was utilized to separate peptide-conjugated SH3 protein from the unconjugated one and the extent of the reaction quantified based on the intensity of Coomassie Blue staining.

ASSOCIATED CONTENT

Supporting Information

Materials and instruments, the general procedure of peptide synthesis, purification and characterization, information on plasmid construction, protein expression and purification, the general procedure of the conjugation reactions, SDS−PAGE, MALDI-TOF analysis of the complexes, and additional characterization data. The Supporting Information is available free of charge on the ACS Publications website at DOI: 10.1021/acs.bioconjchem.5b00238.

AUTHOR INFORMATION

Corresponding Authors

*Phone: 852-3943-6165 . Fax: 852-2603-5057. E-mail: feiye@ust.hk.

*E-mail: jiangxia@cuhk.edu.hk.

Notes

The authors declare no competing financial interest.

ACKNOWLEDGMENTS

We acknowledge Éloïse Peltier for proofreading and polishing the manuscript. Financial support for this work came from the University Grants Committee of Hong Kong (ECS grant CUHK 404812, GRF grants 403711 and 404413, and AoE/M-09/12).

DOI: 10.1021/acs.bioconjchem.5b00238
Bioconjugate Chem. 2015, 26, 1613−1622

REFERENCES

(1) Hermanson, G. T. (2008) *Bioconjugate Techniques*, 2nd edition, Academic Press: London.
(2) Kraut, J. (1977) Serine proteases: structure and mechanism of catalysis. *Annu. Rev. Biochem. 46*, 331−358.
(3) Wang, J., Yu, Y., and Xia, J. (2014) Short peptide tag for covalent protein labeling based on coiled coils. *Bioconjugate Chem. 25*, 178−187.
(4) Lu, Y., Huang, F., Wang, J., and Xia, J. (2014) Affinity-guided covalent conjugation reactions based on PDZ-peptide and SH3-peptide interactions. *Bioconjugate Chem. 25*, 989−999.
(5) Chmura, A. J., Orton, M. S., and Meares, C. F. (2001) Antibodies with infinite affinity. *Proc. Natl. Acad. Sci. U. S. A. 98*, 8480−8484.
(6) Corneillie, T. M., Whetstone, P. A., Lee, K. C., Wong, J. P., and Meares, C. F. (2004) Converting weak binders into infinite binders. *Bioconjugate Chem. 15*, 1389−1391.
(7) Gallagher, S. S., Sable, J. E., Sheetz, M. P., and Cornish, V. W. (2009) An In Vivo covalent TMP-tag based on proximity-induced reactivity. *ACS Chem. Biol. 4*, 547−556.
(8) Nonaka, H., Tsukiji, S., Ojida, A., and Hamachi, I. (2007) Nonenzymatic covalent protein labeling using a reactive tag. *J. Am. Chem. Soc. 129*, 15777−15779.
(9) Nelson, D. L., and Cox M. M. (2004) *Lehninger Principles of Biochemistry*, 4th ed., Palgrave Macmillan: London.
(10) Finn, R. D., Bateman, A., Clements, J., Coggill, P., Eberhardt, R. Y., Eddy, S. R., Heger, A., Hetherington, K., Holm, L., Mistry, J., et al. (2014) Pfam: the protein families database. *Nucleic Acids Res. 42*, 222−230.
(11) Pisabarro, M. T., Serrano, L., and Wilmanns, M. (1998) Crystal structure of the Abl-SH3 domain complexed with a designed high-affinity peptide ligand: implications for SH3-ligand interactions. *J. Mol. Biol. 281*, 513−521.
(12) Jones, M. W., Mantovani, G., Blindauer, C. A., Ryan, S. M., Wang, X., Brayden, D. J., and Haddleton, D. M. (2012) Direct peptide bioconjugation/PEGylation at tyrosine with linear and branched polymeric diazonium salts. *J. Am. Chem. Soc. 134*, 7406−7413.
(13) Gavrilyuk, J., Ban, H., Nagano, M., Hakamata, W., and Barbas, C. F. (2012) Formylbenzene diazonium hexafluorophosphate reagent for tyrosine-selective modification of protains and the introduction of a bioorthogonal aldehyde. *Bioconjugate Chem. 23*, 2321−2328.
(14) Schlich, T. L., Ding, Z., Kovacs, E. W., and Francis, M. B. (2005) Dual-surface modification of the Tobacco Mosaic virus. *J. Am. Chem. Soc. 127*, 3718−3723.
(15) Hooker, J. M., Kovacs, E. W., and Francis, M. B. (2004) Interior surface modification of bacteriophage MS2. *J. Am. Chem. Soc. 126*, 3718−3719.
(16) Chen, S., and Tsao, M. (2013) Genetic incorporation of a 2-Naphthol group into proteins for site-specific Azo coupling. *Bioconjugate Chem. 24*, 1645−1649.
(17) Patai, S. (1978) *The Chemistry of Diazonium and Diazo Groups, Part 1*, John Wiley & Sons Ltd.: New York.
(18) Honda, S., Yamasaki, K., Sawada, Y., and Morii, H. (2004) 10 residue folded peptide designed by segment statistics. *Structure 12*, 1507−1518.
(19) Fedorov, D. G., Ishida, T., Uebayasi, M., and Kitaura, K. (2007) The fragment molecular orbital method for geometry optimizations of polypeptides and proteins. *J. Phys. Chem. A 111*, 2722−2732.
(20) Matthes, D., and de Groot, B. L. (2009) Secondary structure propensities in peptide folding simulations: a systematic comparison of molecular mechanics interaction schemes. *Biophys. J. 97*, 599−608.
(21) Terada, T., Satoh, D., Mikawa, T., Ito, Y., and Shimizu, K. (2008) Understanding the roles of amino acid residues in tertiary structure formation of chignolin by using molecular dynamics simulation. *Proteins: Struct., Funct., Genet. 73*, 621−631.
(22) Suenaga, A., Narumi, T., Futatsugi, N., Yanai, R., Ohno, Y., Okimoto, N., and Taiji, M. (2007) Folding dynamics of 10-residue beta-hairpin peptide chignolin. *Chem. - Asian J. 2*, 591−598.
(23) Verhelst, S. H. L., Fonović, and Bogyo, M. (2007) A mild chemically cleavable linker system for functional proteomic applications. *Angew. Chem., Int. Ed. 46*, 1284−1286.
(24) Heal, W. P., and Tate, E. W. (2010) Getting a chemical handle on protein post-translational modification. *Org. Biomol. Chem. 8*, 731−738.
(25) Cicchetti, P., Mayer, B. J., Thiel, G., and Baltimore, D. (1992) Identification of a protein that binds to the SH3 region of Abl and is similar to Bcr and GAP-rho. *Science 257*, 803−806.
(26) Panjarian, S., Iacob, R. E., Chen, S., Engen, J. R., and Smithgall, T. E. (2013) Structure and dynamic regulation of Abl kinases. *J. Biol. Chem. 288*, 5443−5450.
(27) Saksela, K., and Permi, P. (2012) SH3 domain ligand binding: what's the consensus and where's the specificity? *FEBS Lett. 586*, 2609−2614.
(28) Mayer, B. J., and Eck, M. J. (1995) Minding your p's and q's. *Curr. Biol. 5*, 364−367.
(29) Palencia, A., Camara-Artigas, A., Pisabarro, M. T., Martinez, J. C., and Luque, I. (2010) Role of interfacial water molecules in proline-rich ligand recognition by the Src Homology 3 domain of Abl. *J. Biol. Chem. 285*, 2823−2833.
(30) Palencia, A., Cobos, E. S., Mateo, P. L., Martínez, J. C., and Luque, I. (2004) Thermodynamic dissection of the binding energetics of proline-rich peptides to the Abl-SH3 domain: implications for rational ligand design. *J. Mol. Biol. 336*, 527−537.
(31) Pisabarro, M. T., and Serrano, L. (1996) Rational design of specific high-affinity peptide ligands for the Abl-SH3 domain. *Biochemistry 35*, 10634−10640.
(32) Farrera-Sinfreu, J., Giralt, E., Castel, S., Albericio, F., and Royo, M. (2005) Cell-penetrating *cis-gama*-amino-L-proline-derived peptides. *J. Am. Chem. Soc. 127*, 9459−9468.
(33) Horne, W. S. (2011) Peptide and peptoid foldamers in medicinal chemistry. *Expert Opin. Drug Discovery 6*, 1247−1262.
(34) Zhang, W., Sun, F., Tirrell, D. A., and Arnold, F. H. (2013) Controlling macromolecular topology with genetically encoded SpyTag-SpyCatcher chemistry. *J. Am. Chem. Soc. 135*, 13988−13997.
(35) Zakeri, B., Fierer, J. O., Celik, E., Chittock, E. C., Schwarz-Linek, U., Moy, V. T., and Howarth, M. (2012) Peptide tag forming a rapid covalent bond to a protein, through engineering a bacterial adhesin. *Proc. Natl. Acad. Sci. U. S. A. 109*, E690−E697.
(36) Schoene, C., Fierer, J. O., Bennett, S. P., and Howarth, M. (2014) SpyTag/SpyCatcher cyclization confers resilience to boiling on a mesophilic enzyme. *Angew. Chem., Int. Ed. 53*, 6101−6104.
(37) Chen, Z., Popp, B. V., Bovet, C. L., and Ball, Z. T. (2011) Site-specific protein modification with a dirhodium metallopeptide catalyst. *ACS Chem. Biol. 6*, 920−925.
(38) Popp, B. V., and Ball, Z. T. (2010) Structure-selective modification of aromatic side chains with dirhodium metallopeptide catalysts. *J. Am. Chem. Soc. 132*, 6660−6662.
(39) Ball, Z. T. (2015) Molecular recognition in protein modification with rhodium metallopeptides. *Curr. Opin. Chem. Biol. 25*, 98−102.
(40) Tsukiji, S., Miyagawa, M., Takaoka, Y., Tamura, T., and Hamachi, I. (2009) Ligand-directed tosyl chemistry for protein labeling in vivo. *Nat. Chem. Biol. 5*, 341−343.
(41) Takahashi, M., Kawamura, A., Kato, N., Nishi, T., Hamachi, I., and Ohkanda, J. (2012) Phosphopeptide-dependent labeling of 14−3−3ζ proteins by fusicoccin-based fluorescent probes. *Angew. Chem., Int. Ed. 51*, 509−512.
(42) Koshi, Y., Nakata, E., Miyagawa, M., Tsukiji, S., Ogawa, T., and Hamachi, I. (2008) Target-Specific Chemical Acylation of Lectins by Ligand-Tethered DMAP Catalysts. *J. Am. Chem. Soc. 130*, 245−251.
(43) Wang, H., Koshi, Y., Minato, D., Nonaka, H., Kiyonaka, S., Mori, Y., Tsukiji, S., and Hamachi, I. (2011) Chemical Cell-Surface Receptor Engineering Using Affinity-Guided, Multivalent Organocatalysts. *J. Am. Chem. Soc. 133*, 12220−12228.
(44) Sato, S., and Nakamura, H. (2013) Ligand-directed selective protein modification based on local single-electron-transfer catalysis. *Angew. Chem., Int. Ed. 52*, 8681−8684.

DOI: 10.1021/acs.bioconjchem.5b00238
Bioconjugate Chem. 2015, 26, 1613−1622

(45) Holm, L., Moody, P., and Howarth, M. (2009) Electrophilic affibodies forming covalent bonds to protein targets. *J. Biol. Chem. 284*, 32906−32913.
(46) Gushwa, N. N., Kang, S., Chen, J., and Taunton, J. (2012) Selective targeting of distinct active site nucleophiles by irreversible Src-family kinase inhibitors. *J. Am. Chem. Soc. 134*, 20214−20217.
(47) Delaglio, F., Grzesiek, S., Vuister, G. W., Zhu, G., Pfeifer, J., and Bax, A. (1995) NMRPipe: a multidimensional spectral processing system based on UNIX pipes. *J. Biomol. NMR 6*, 277−293.
(48) Goddard, T. D., and Kneller, D. G. (2008) *SPARKY 3*, University of California: San Francisco, CA.
(49) Schägger, H. (2006) Tricine-SDS-PAGE. *Nat. Protoc. 1*, 16−22.

DOI: 10.1021/acs.bioconjchem.5b00238
Bioconjugate Chem. 2015, 26, 1613−1622